



This is a repository copy of *A photosynthetic antenna complex foregoes unity carotenoid-to-bacteriochlorophyll energy transfer efficiency to ensure photoprotection.*

White Rose Research Online URL for this paper:  
<http://eprints.whiterose.ac.uk/159632/>

Version: Accepted Version

---

**Article:**

Niedzwiedzki, D.M., Swainsbury, D.J.K. [orcid.org/0000-0002-0754-0363](https://orcid.org/0000-0002-0754-0363), Canniffe, D.P. et al. (2 more authors) (2020) A photosynthetic antenna complex foregoes unity carotenoid-to-bacteriochlorophyll energy transfer efficiency to ensure photoprotection. *Proceedings of the National Academy of Sciences*, 117 (12). pp. 6502-6508. ISSN 0027-8424

<https://doi.org/10.1073/pnas.1920923117>

---

© 2020 The Author(s) Published under the PNAS license. This is an author-produced version of a paper subsequently published in *Proceedings of the National Academy of Sciences*. Uploaded in accordance with the publisher's self-archiving policy.

**Reuse**

Items deposited in White Rose Research Online are protected by copyright, with all rights reserved unless indicated otherwise. They may be downloaded and/or printed for private study, or other acts as permitted by national copyright laws. The publisher or other rights holders may allow further reproduction and re-use of the full text version. This is indicated by the licence information on the White Rose Research Online record for the item.

**Takedown**

If you consider content in White Rose Research Online to be in breach of UK law, please notify us by emailing [eprints@whiterose.ac.uk](mailto:eprints@whiterose.ac.uk) including the URL of the record and the reason for the withdrawal request.



[eprints@whiterose.ac.uk](mailto:eprints@whiterose.ac.uk)  
<https://eprints.whiterose.ac.uk/>

**Classification: Biological Sciences (Biochemistry)**

**A photosynthetic antenna complex foregoes unity carotenoid to bacteriochlorophyll energy transfer efficiency to ensure photoprotection**

Dariusz M. Niedzwiedzki<sup>1,2,\*</sup>, David J.K. Swainsbury<sup>3</sup>, Daniel P. Canniffe<sup>4</sup>, C. Neil Hunter<sup>3</sup> and Andrew Hitchcock<sup>3,\*</sup>

<sup>1</sup>Center for Solar Energy and Energy Storage, Washington University in St. Louis, St. Louis, MO 63130 USA

<sup>2</sup>Department of Energy, Environmental & Chemical Engineering, Washington University in St. Louis, St. Louis, MO 63130 USA

<sup>3</sup>Department of Molecular Biology and Biotechnology, University of Sheffield, Sheffield, S10 2TN, United Kingdom

<sup>4</sup>Institute of Integrative Biology, University of Liverpool, L69 7ZB, United Kingdom

**\*Corresponding Authors:** Dr. Dariusz M. Niedzwiedzki, Washington University, St. Louis, MO 63130 USA. Phone: +1(314)9358483. E-mail: niedzwiedzki@wustl.edu; Dr. Andrew Hitchcock, University of Sheffield, Sheffield, S10 2TN, UK. Phone: +44(0)1142224240. Email: a.hitchcock@sheffield.ac.uk

**Author ORCID IDs:** Dariusz M. Niedzwiedzki: 0000-0002-1976-9296; David J.K. Swainsbury: 0000-0002-0754-0363; Daniel P. Canniffe: 0000-0002-5022-0437; C. Neil Hunter: 0000-0003-2533-9783; Andrew Hitchcock: 0000-0001-6572-434X.

**Keywords:** photosynthesis, carotenoids, light harvesting, photoprotection, ultrafast spectroscopy

## Abstract

Carotenoids serve a dual purpose in photosynthesis, providing light-harvesting and photoprotective energy dissipation functions within pigment-protein complexes. The carbon-carbon double bond (C=C) conjugation length of carotenoids ( $N$ ), generally between 9 and 15, determines the carotenoid-to-(bacterio)chlorophyll ((B)Chl) energy transfer efficiency. Here, we purified and spectroscopically characterized light harvesting complex 2 (LH2) from *Rhodospira rubra* containing the  $N = 7$  carotenoid zeta ( $\zeta$ )-carotene, not previously incorporated within an antenna complex. Transient absorption and time-resolved fluorescence show that, relative to the lifetime of the  $S_1$  state of  $\zeta$ -carotene in solvent, the lifetime decreases  $\sim 250$ -fold when  $\zeta$ -carotene is incorporated within LH2, due to transfer of excitation energy to the B800 and B850 BChls a. These measurements show that energy transfer proceeds with an efficiency of  $\sim 100\%$ , primarily via the  $S_1 \rightarrow Q_x$  route because the  $S_1 \rightarrow S_0$  fluorescence emission of  $\zeta$ -carotene overlaps almost perfectly the  $Q_x$  absorption band of the BChls. However, transient absorption measurements performed on microsecond timescales reveal that, unlike the native  $N \geq 9$  carotenoids normally utilized in light-harvesting complexes,  $\zeta$ -carotene does not quench excited triplet states of BChl a, likely due to elevation of the  $\zeta$ -carotene triplet energy state above that of BChl a. These findings provide insights into the co-evolution of photosynthetic pigments and pigment-protein complexes. We propose that the  $N \geq 9$  carotenoids found in light-harvesting antenna complexes represent a vital compromise that retains an acceptable level of energy transfer from carotenoids to (B)Chls while allowing acquisition of a new, essential function, namely photoprotective quenching of harmful (B)Chl triplets.

### **Significance statement**

Photosynthesis uses carotenoids as light-harvesting pigments and for photoprotective energy dissipation. The carbon–carbon double bond conjugation length of carotenoids ( $N$ ) affects the carotenoid-to-(bacterio)chlorophyll energy transfer efficiency but the photoprotective capability was considered to be independent of  $N$ . Using light-harvesting complex 2 from the model photosynthetic bacterium *Rhodobacter sphaeroides* containing  $\zeta$ -carotene ( $N = 7$ ) or neurosporene ( $N = 9$ ), we demonstrate that decreasing the conjugation length increases the carotenoid-to-bacteriochlorophyll energy transfer efficiency, in the case of  $\zeta$ -carotene to approximately 100%. However, unity quantum efficiency comes at the cost of photoprotection, suggesting that naturally evolved photosynthesis tolerates some energetic loss to allow essential energy dissipation, explaining why longer conjugation length carotenoids are utilized in native pigment-protein complexes.

### **Author contributions**

D.M.N. and A.H. designed research; D.M.N., D.J.K.S., D.P.C. and A.H. performed research. All authors analyzed data and wrote the paper.

### **Conflict of interest statement**

The authors declare no competing interest.

## Introduction

Carotenoids (Cars) are natural pigments found in plants, algae and photosynthetic (cyano)bacteria where they function in light harvesting, stabilization of pigment-protein complex structure and photoprotection (1, 2). In antenna complexes and photosystems Cars act as accessory light-harvesting pigments and transfer excitation energy to (bacterio)chlorophylls ((B)Chls). The absorption band of Cars typically spans the 400-550 nm spectral range and is associated with the  $S_0 \rightarrow S_2$  electronic transition of the linear carbon-carbon double bond (C=C) conjugation (N), a characteristic structural motif (3, 4). Cars also have an important photoprotective functions in light-harvesting complexes, typically quenching harmful excited triplet states of (B)Chls to inhibit formation of reactive oxygen species such as singlet oxygen (5). The photophysical properties of Cars and their roles in numerous light harvesting antennae have been investigated (6). The LH2 complex from purple photosynthetic bacteria has been a model antenna for such studies (7-16) as crystal structures are available (17, 18), the Car content can be manipulated (14, 19-22), and its relatively simple pigment composition reduces the number of features that must be interpreted in spectroscopic analyses.

Numerous studies have shown that the Car-to-BChl a energy transfer efficiency ( $\Phi_{\text{Car} \rightarrow \text{BChl}}$ ) varies in LH2s from different purple bacterial species and appears to correlate with the Car conjugation length. The yields for Cars such as neurosporene (N = 9) or spheroidene (N = 10) are 85-95% (11, 19, 23-25). The yields decrease to 55–65% for Cars where N = 11 (e.g. rhodopin, rhodopin glucoside or lycopene) (11, 24-26) and reduce further to ~30% when N = 13 (spirilloxanthin) (14). As longer C=C conjugation length (larger N) lowers the energies of both the  $S_2$  and  $S_1$  excited states (2, 6), the broadly accepted explanation for the variation in  $\Phi_{\text{Car} \rightarrow \text{BChl}}$

in LH2 is linked with the inherent excited-state properties of the particular Car. Typically, both  $S_2$  and  $S_1$  states are involved in energy transfer to BChls and if the  $S_1$  state falls below the  $Q_y$  bands of the B800 and B850 spectral forms of BChl a, reducing spectral overlap of the hypothetical  $S_1$  emission and BChl a absorption, then the  $\Phi_{\text{Car} \rightarrow \text{BChl}}$  declines sharply. At first glance some Cars do not appear to fit into this correlation, for example okenone with  $N = 13 + \text{C}=\text{O}$ , where nominally there are 13 conjugated carbon-carbon bonds and a terminal  $\text{C}=\text{O}$  group that could extend the conjugation length. Okenone bound within the LH2 complex from the bacterium *Merichromatium purpuratum* (formerly *Chromatium purpuratum*) shows  $\Phi_{\text{Car} \rightarrow \text{BChl}} = 85.6\%$  (27), substantially above the expected value of  $\sim 30\%$  observed for other  $N = 13$  Cars. However, previous investigations have demonstrated that when conjugation is extended into the cyclic ends of Cars the double bonds in the rings act as only  $\sim 0.3$  of a double bond in the linear backbone, and in case of Cars with aryl rings such as okenone the contribution may be even smaller (28, 29). Indeed, it has been shown that the energies of the excited states of okenone are only marginally smaller than their counterparts for the open chain Car spheroidenone ( $N = 10 + \text{C}=\text{O}$ ) (30), which when bound to LH2 shows a  $\Phi_{\text{Car} \rightarrow \text{BChl}}$  of 92-94% (11, 20), similar to that of okenone.

Unlike  $\Phi_{\text{Car} \rightarrow \text{BChl}}$  efficiency, the ability to provide photoprotective quenching of BChl a excited states (triplets) is more or less the same for all of the above mentioned Cars incorporated into LH2 (7, 31, 32). It could therefore be perceived that the ability to photoprotect (B)Chls in photosynthetic antennas is a universal characteristic of all Cars, however this is not the case. Energetic requirements between (B)Chl and Car triplet states must also be considered and, like the  $S_2$  and  $S_1$  states, the triplet states of Cars have well-defined energies that also depend on  $N$ ,

although this is impossible to directly confirm due to undetectable phosphorescence. Interestingly, photosynthetic organisms have a strong preference for Cars with  $N \geq 9$  for incorporation into light-harvesting proteins (1), suggesting that Cars with  $N \geq 9$  have triplet state energies in a “sweet spot” corresponding to the triplet state energies of specific (B)Chls to ensure the most efficient sensitization ((B)Chls triplet quenching) (33). In support of this idea, experiments that tested photoprotective abilities of open chain and cyclic Cars of different  $N$  lengths in Car-Chl a model mixtures demonstrated that photoprotective capability appear to falls sharply for Cars with  $N \leq 8$  (34-36).

Here we set out to better understand the relationship between Car conjugation length, Car-to-BChl energy transfer efficiency, and Car photoprotective ability using LH2 complexes from the model purple phototrophic bacterium *Rba. sphaeroides* containing either neurosporene ( $N = 9$ ) or zeta ( $\zeta$ )-carotene ( $N = 7$ ). Using this model antenna we provide direct evidence that Cars with a conjugation length of only 7 are fully efficient in Car-to-BChl a energy transfer, but are unable to quench excited states of BChl a, a conflict that could have influenced the evolution of a compromise between energy transfer and photoprotection in photosynthetic light-harvesting complexes from other organisms.

## **Results**

### **$\zeta$ -carotene to BChl a energy transfer in LH2 proceeds with unity quantum efficiency**

We performed comparative spectroscopic studies of  $\zeta$ -carotene bound to LH2 (see Materials and Methods, SI Appendix, figure S1 for details of the  $\zeta$ -carotene producing strain of *Rba.*

sphaeroides and purification of LH2) and isolated  $\zeta$ -carotene in solvent; steady-state absorption in both environments and fluorescence emission spectrum of  $\zeta$ -carotene in solvent and in LH2 are shown in Figure 1. The absorption spectrum of LH2-bound  $\zeta$ -carotene shows two clearly pronounced vibronic bands at 441 and 413 nm. The near-perfect overlap of the absorbance (1-transmittance) and the fluorescence excitation spectrum when monitoring emission exclusively from BChl a shows that  $\zeta$ -carotene is a perfect excitation energy donor to BChl a with  $\Phi_{\text{Car} \rightarrow \text{BChl}} \sim 100\%$  (Figure 1A). This ideal  $\Phi$  value suggests that there are no additional processes competing with energy transfer (ET), such as triplet formation via singlet fission or formation of a Car cation, which reduces  $\Phi_{\text{Car} \rightarrow \text{BChl}}$  by 5–15% for Cars with longer N values (11, 21, 37). Examination of the spectra reveals that the  $S_2$  excited state is too far from the  $Q_x$  absorption resulting in insufficient overlap to permit  $S_2 \rightarrow Q_x$  energy transfer. Transfer from  $S_2 \rightarrow Q_x$  is typical for Cars with longer conjugations (i.e.  $S_2$  energies red shifted relative to that of  $\zeta$ -carotene) (10), therefore it is possible that the majority of the ET occurs from the  $S_1$  excited state. It is broadly accepted that LH2 complexes bind Cars in all-trans geometry (17) and for comparative studies with isolated Car in solvent we purified the all-trans geometric isomer of  $\zeta$ -carotene (the purification procedure is described in SI Appendix, Figure S2). To examine the intrinsic properties of the all-trans- $\zeta$ -carotene  $S_1$  state, we combined steady-state and time-resolved fluorescence measurements with transient absorption spectroscopy. As demonstrated in Figure 1B, the Car dissolved in solvent has detectable fluorescence. We assign the main band between 550 and 700 nm as emission from the  $S_1 \rightarrow S_0$  transition and the smaller band at  $\sim 480$  nm as emission from  $S_2 \rightarrow S_0$ . Generally, Cars are known to have very low fluorescence quantum yields, therefore the fluorescence spectrum could easily be overwhelmed by sample



contaminants. To ensure that the emission is associated with the Car fluorescence the excitation spectrum was measured (Figure 1B red dash-dot line). The very good agreement with the absorbance (1-transmittance) spectrum of all-trans- $\zeta$ -carotene confirms that the observed emission is that of the  $S_1 \rightarrow S_0$  fluorescence emission of the Car.

### **$\zeta$ -carotene to BChl a energy transfer proceeds from the $S_1$ excited singlet state**

The fluorescence spectra show that emission from the  $S_1$  and  $S_2$  transitions partially overlap and it is uncertain if the vibronic band at ~550 nm originates from the  $S_1$  excited state (0-0 vibronic band) or if an additional peak at shorter wavelengths is obscured by the tail of the  $S_2$  state emission. Using time-resolved fluorescence (TRF) of the Car, as shown by the pseudo-color 2D fluorescence decay contour map in Figure 2A, we could unambiguously assign these features. It is clear that both emissive transitions are temporally resolved. What is not apparent from the contour is that there is a weaker, longer-lived band with a maximum at ~550 nm that is likely associated with emission from sample contaminants, which may form and accumulate during laser exposure. Global analysis of the TRF data was used to temporally and spectrally separate emission bands; Figure 2B shows these results along with the kinetic scheme used for fitting. The fitting results (SAS – species associated spectra) reflect emission from the excited states of Car and sample contaminants. Fitting shows that the intrinsic lifetime of the  $S_1$  state is 340 ps. The quality of the fit is shown in Figure 2C, which contains the fluorescence decay profiles for the  $S_1$  and  $S_2$  states together with fits from global analysis. In order to obtain the  $S_1$  state energy from the fluorescence emission, the 340 ps SAS was subjected to a simulation of the vibronic progression with Franck-Condon (FC) factors according to a simplified formula that assumed

only one average vibronic mode  $\langle \nu \rangle$  contributing to the spectrum with an average displacement  $\langle \Delta \rangle$  between the state coordinates (Figure 2D) (see Materials and Methods for more details):

$$FC(\nu) = C\nu \sum_v \frac{\langle \Delta \rangle^{2v}}{2^v v!} \exp\left(-\frac{\langle \Delta \rangle^2}{2}\right) \frac{1}{2\pi\sigma} \exp\left(-\frac{[\nu - (\nu_{00} - \nu(\nu))]^2}{2\sigma^2}\right) \quad (1)$$

The simulated spectrum (red line) was obtained based on the following parameters:  $\nu = 6$  (number of vibronic bands),  $\langle \Delta \rangle = 2.21$ ,  $\langle \nu \rangle = 1,120 \text{ cm}^{-1}$ ,  $\nu_{00} = 17,980 \text{ cm}^{-1}$  (energy of the  $S_1$  state),  $\sigma = 540 \text{ cm}^{-1}$  (width of the vibronic band in  $\text{cm}^{-1}$ ),  $C = 72$  (arbitrary scaling constant).

To permit comparison with the LH2-bound Car, the excited state lifetime of all-trans- $\zeta$ -carotene in solvent was also determined by transient absorption (TA) spectroscopy. The TA results obtained at room temperature and 77 K, along with an expanded description, are provided in Figure S3. Fitting of the TA data gives an  $S_1$  state lifetime of 340 ps, in excellent agreement with TRF measurements despite the vastly different temporal resolutions of the two methods. The extensive overlap of the  $\zeta$ -carotene emission spectrum with the 600 nm BChl a  $Q_x$  absorption, combined with its strong fluorescence emission (i.e. high quantum yield) and long  $S_1$  excited state lifetime, should make  $\zeta$ -carotene an ideal accessory light-harvesting pigment. We predict that  $\zeta$ -carotene will perform better than its counterparts with longer conjugations such as neurosporene ( $N = 9$ ) or spheroidene ( $N = 10$ ), which show much weaker, almost undetectable  $S_1 \rightarrow S_0$  fluorescence emission and have no spectral overlap with the BChl a  $Q_x$  band (38).

### **Transfer dynamics of the Car $S_1 \rightarrow$ BChl a $Q_x$ excitation energy transfer**

To determine the excited state properties of  $\zeta$ -carotene bound within LH2, transient absorption spectroscopy was applied to the entire complex allowing simultaneous measurement of  $\zeta$ -

carotene and the energy-accepting BChls (Figure 3). Figure 3A shows a pseudo-color 2D contour map measured between 330 and 910 nm over 1300 ps plotted on a semi-logarithmic time axis for better visibility of the transient bands. A subset of representative TA spectra taken at various times after excitation are shown in Figure 3B and dynamics at chosen wavelengths are shown in Figure 3C. It is evident that the excited state absorption (ESA) band associated with the  $S_1$  state (positive band at 489 nm) decays almost entirely within 4 ps. Given that the  $S_1$  state lifetime in solvent is 340 ps, this dramatic reduction shows the high efficiency of the  $S_1 \rightarrow Q_x$  route in the energy transfer process.

More details of the ET dynamics were revealed with global analysis of the TA data provided in Figure 3D. Fitting was performed according to a sequential pathway of excitation decay and migration (irreversible steps from the fastest to the slowest lifetimes) to generate evolution associated decay spectra (EADS). This analysis does not necessarily reproduce the transient spectra of each species in the pathway but it is satisfactory for obtaining macroscopic rates (observed lifetimes) of each distinct spectral component. These EADS can be interpreted by comparison with previous studies of other LH2 complexes. The EADS with lifetime of 220 fs can be assigned to decay of the initially excited  $\zeta$ -carotene  $S_2$  state. The lifetime is similar to the  $S_2$  lifetime observed in solvent at room temperature (SI Appendix, Figure S3), which suggests that there is negligible ET to BChl a, and the excitation internally converts to the  $S_1$  state. The  $S_1$  state has a lifetime of 1.37 ps, ~250-fold less than the 340 ps lifetime in solvent, confirming that it participates in extremely efficient ET to the  $Q_x$  bands of both the B800 and B850 spectral forms of BChl a as demonstrated by simultaneous bleaching of the B800 and B850 bands associated with depletion of BChls in the ground state. Two EADS are associated with BChls,

the B800\* $\rightarrow$ B850 energy transfer at 4.9 ps (following excitation of the B800 BChl a from the Car S<sub>1</sub> state) and the decay of the excited B850 BChl a at 850 ps, for which the excited state lifetime is known to be ~1000 ps (22, 31, 32, 37).

### **$\zeta$ -carotene is not a quencher of BChl a triplets**

Figure 3D shows a fifth EADS with an infinite (inf) lifetime, meaning it belongs to a process that is far slower than the 7 ns measurement time window. The long lifetime and spectral shape suggest that it is associated with the B850 BChl a triplet, formed by inter-system crossing (ISC) at an efficiency of ~30% (32). The presence of this component is interesting because it is well established that B850 BChl a triplets are rapidly quenched by sensitization of Car triplets, at most within a few tens of nanoseconds of formation, preventing their accumulation (31, 32). The accumulation of BChl a triplets is potentially damaging as they may sensitize harmful singlet oxygen, whereas Car triplets are harmless as the triplet energy safely dissipates as heat. Therefore, triplet quenching by Cars provides an essential photoprotective function. Here, the presence of a kinetic component corresponding to long-lived B850 BChl a triplets suggests that this essential photoprotective mechanism is absent in LH2 complexes containing  $\zeta$ -carotene. To test this hypothesis the LH2 complexes with  $\zeta$ -carotene and a second control LH2 complex containing neurosporene (N = 9) were studied by TA in the microsecond time domain (Figure 4). The control LH2 was isolated from a  $\Delta$ crtC mutant of *Rba. sphaeroides*, described previously (19). Figure 4A, B shows 2D-pseudocolor TA contours with transient bands marked with arrows. These are accompanied by selected TA spectra (Figure 4C and D) at various delay times after excitation, with inset panels showing the spectral range of the Car triplet transient band. It is apparent that for the  $\zeta$ -carotene-containing LH2 the Car triplet spectrum is absent, whereas it can

be clearly seen for the control complex with neurosporene. Conversely the triplet state of B850 is long-lived in the  $\zeta$ -carotene-containing complex, whereas it completely decays within  $\sim 70$  ns in the neurosporene-containing LH2. Taken together these data show that in the  $\zeta$ -carotene-containing LH2 the B850 BChl a triplet state is not quenched by formation of a Car triplet, whereas Car triplet formation is observed in the control neurosporene-containing LH2 sample (compare Figure 4E and F).

## Discussion

This study provides direct evidence that Cars with shorter conjugation lengths (here  $N = 7$ ) are unable to participate in the essential function of photoprotection in a model bacterial light harvesting complex. Triplet state energies of monomeric (B)Chls are already well defined and depending on the (B)Chl species span an energetic range of  $8,000\text{--}10,750\text{ cm}^{-1}$  ( $930\text{--}1250\text{ nm}$ ). All these triplet states lie above the  $7,870\text{ cm}^{-1}$  ( $1,270\text{ nm}$ ) energy level of singlet oxygen (33), making them efficient sensitizers of this harmful product. Although the triplet energies of Cars cannot be measured directly due to a lack of spectral features, they can be inferred by their interactions with observable triplets of other molecules. Specifically, the triplet state of BChl a is  $\sim 8,200\text{ cm}^{-1}$  ( $1,220\text{ nm}$ ), marginally above singlet oxygen (33). Because Cars with  $N \geq 9$  efficiently quench BChl a, this strongly suggests that they also have triplet energies below that of singlet oxygen, allowing efficient and harmless BChl a triplet quenching, as observed here in LH2 containing neurosporene. However, Cars with  $N \leq 7$  are likely to have triplet energies above BChl a rendering triplet exchange to the Car energetically unfavorable, as observed here for LH2

containing  $\zeta$ -carotene. In the absence of quenching, long-lived BChl a triplets will sensitize singlet oxygen leading to oxidative damage of the cell.

So what is the situation with Cars and N in other photosynthetic antenna complexes that use different species of B(Chl) for light-harvesting? As discussed above, the triplet state energy levels of the various (B)Chls that exist in nature span a broad energetic range, thus the “cut-off” conjugation length at which Cars lose their photoprotective function in respect to a specific (B)Chl species may not be strictly limited to  $N = 7$  in other light-harvesting complexes. However, because the triplet state of BChl a is energetically only marginally higher than that of singlet oxygen, the lack of quenching of BChl a triplets by  $\zeta$ -carotene strongly suggests that the energy of the triplet state of  $\zeta$ -carotene is higher than the energy level of singlet oxygen. Consequently, employing a Car with  $N = 7$  (or less) in any LH complex is unlikely to be beneficial as even if the Car can quench a specific (B)Chl triplet, it will in turn become a singlet oxygen sensitizer itself.

In summary, our study provides an evolutionary insight into the coevolution of photosynthetic pigment-protein complexes and BChl a and Car biosynthesis. Despite Cars with shorter conjugation length being simpler for the organism to produce and able to transfer energy to (B)Chls with increased quantum efficiency, below a certain N value the inability to provide photoprotection of harmful B(Chl) excited states suggests it is not coincidental that all antenna complexes of photosynthetic organisms utilize Cars with  $N \geq 9$ .

## **Materials and Methods**

### **Growth of *Rba. sphaeroides* and generation of a $\zeta$ -carotene producing strain**

Liquid cultures of *Rba. sphaeroides* were grown in M22+ medium (39) supplemented with 0.1% (w/v) casamino acids. For microoxic growth cultures were shaken at 175 rpm at 30 °C. Phototrophic growth was performed in completely full culture vessels agitated with magnetic stir bars under  $\sim 50 \mu\text{mol photons m}^{-2} \text{ s}^{-1}$  illumination provided by OSRAM classic 116 W halogen bulbs. Medium was supplemented with  $30 \mu\text{g ml}^{-1}$  kanamycin and/or 10% (w/v) sucrose as appropriate.

The neurosporene-accumulating  $\Delta\text{crtC}$  and phytoene-accumulating  $\Delta\text{crtI}$  strains of *Rba. sphaeroides* 2.4.1 have been described previously (19); the *crtC* gene (*rsp\_0267*) was deleted from the  $\Delta\text{crtI}$  mutant using the pK18mobsacB allelic exchange construct described in the same study. The plasmid was conjugated into the  $\Delta\text{crtI}$  strain from *Escherichia coli* S17-1 with selection on M22+ agar containing kanamycin. Subsequent plating on M22+ agar containing sucrose isolated colonies where the plasmid was excised from the genome and  $\Delta\text{crtC}$  mutants were identified by PCR and verified by automated DNA sequencing.

To produce  $\zeta$ -carotene in *Rba. sphaeroides*, the *Synechocystis* sp. PCC 6803 phytoene desaturase (PDS) encoding gene (*pds*, *slr1254*) was introduced to the  $\Delta\text{crtI}$   $\Delta\text{crtC}$  background. The *pds* gene was amplified from genomic DNA with primers *slr1254\_F* (5'-ACTGAGATCTATGCGCGTTGTGATCGCC-3'; BglII site underlined in italics) and *slr1254\_R* (5'-TCGACTCGAGTTAACCCACGGTGACTATTTCCCTG-3'; XhoI site underlined in italics) using Q5 DNA polymerase (NEB). The resulting 1439 bp PCR product was digested with BglII/XhoI and ligated into the same sites of the replicative pBBRBB-Ppuf843–1200 plasmid such that expression of *pds* is under control of the truncated *puf* promoter (40) The sequence

verified plasmid was conjugated into the  $\Delta$ crtI  $\Delta$ crtC strain of *Rba. sphaeroides* from *E. coli* S17-1 with selection on M22+ agar containing  $30 \mu\text{g ml}^{-1}$  kanamycin.

### **$\zeta$ -carotene extraction and purification**

Pigments (Cars and BChl a) were extracted with acetone and methanol at a 50:50 (v:v) ratio in approximately 10 mL volume. Water (~0.5 mL) was added, followed by approximately 10 mL of petroleum ether. The mixture was agitated and saponified by adding few small pellets of NaOH. Water was added until  $\zeta$ -carotene was fully partitioned into the ether layer, which was carefully removed. The ether was dried down using a stream of nitrogen gas in darkness and the Cars were resuspended in acetone. The mixture of  $\zeta$ -carotene isomers was purified using an Agilent 1100 HPLC system consisting a quaternary pump, in line diode array UV-Vis detector and  $4.6 \times 250$  mm Zorbax Eclipse XBD-C18 column. The flow rate was 1 mL/min, the sample injection volume was 100  $\mu\text{L}$  (in acetone) and the mobile phase was 40:30:30 (v/v/v) acetonitrile:methanol:tetrahydrofuran. All-trans- $\zeta$ -carotene was isolated using a YMC Carotenoid C30 column with the same HPLC system, mobile phase and flow rate (see SI Appendix for more details). All solvents were HPLC grade (Millipore Sigma).

### **Purification of $\zeta$ -carotene or neurosporene containing LH2**

LH2 from the  $\zeta$ -carotene or neurosporene producing strains was purified by ion-exchange and size-exclusion chromatography as described previously (41).

### **Spectroscopic methods**

Room temperature and 77 K steady-state absorption spectra of the LH2 complexes and isolated  $\zeta$ -carotene were recorded using a UV-1800 spectrophotometer (Shimadzu). Fluorescence emission spectra of  $\zeta$ -carotene and the LH2 samples were measured using an RF-6000



spectrofluorometer (Shimadzu) following excitation of the (0-0) vibronic peak of the  $S_0 \rightarrow S_2$  absorption band of the Car dissolved in HPLC eluent (solvent mix; see above) and the Soret band of BChl a (370 nm), respectively. Excitation and emission bandwidths were set to 5 nm and a 455 nm (650 nm) long pass glass filter was used for emission measurements in solvent mix (LH2) at the detector entrance. Fluorescence excitation spectra were collected monitoring emission at 855 nm for LH2 and at 630 nm for the Car in solvent, with excitation and emission bandwidths of 5 nm. To minimize scattering effects, long-pass glass filters were placed at the detector entrance (610 nm for  $\zeta$ -carotene in solvent mix and 780 nm for LH2). Cryogenic measurements at 77 K were carried out using a VNF-100 liquid nitrogen cryostat (Janis).  $\zeta$ -carotene was dissolved in 2-methyltetrahydrofuran (2-MTHF) in a 1 cm cryogenic quartz cuvette (NSG Precision Cells) and slowly frozen in nitrogen vapor to form a transparent glass. For fluorescence studies all samples were adjusted to an absorbance of 0.1 at either the maximum of the  $S_0 \rightarrow S_2$  absorption band ( $\zeta$ -carotene) or the B850 band (LH2).

Transient absorption (TA) experiments were carried out using Helios-EOS, a tandem femtosecond/nanosecond time-resolved pump-probe absorption spectrometer (UltrafastSystems LLC) coupled to a Spectra-Physics femtosecond laser system described in detail previously (42). The LH2 complex was excited at 442 nm corresponding to the (0-0) vibronic peak of the  $\zeta$ -carotene absorption band.  $\zeta$ -carotene in 2-MTHF was excited at 428 nm (RT) or at 439 nm (77 K). The energy of the excitation beam, focused on the sample in a spot of approximately 1 mm diameter, was 200-400 nJ, corresponding to  $6-1 \times 10^{13}$  photons  $\text{cm}^{-2}$  pulse $^{-1}$ .

Time-resolved fluorescence (TRF) imaging was performed using a universal streak camera system from Hamamatsu (Hamamatsu Corporation) equipped with a N51716-04 streak

tube and A6365-01 Bruker spectrograph (Bruker Corporation) and coupled to an ultrafast laser system (Spectra-Physics) (43). The repetition rate of the excitation laser was set to 8 MHz (125 ns between subsequent pulses). The excitation beam was depolarized, focused on the sample in a circular spot of ~1 mm diameter and set to a wavelength of 410 nm (second order harmonics of 820 nm) and a very low photon flux of  $\sim 10^{10}$  photons  $\text{cm}^{-2}$  pulse $^{-1}$ . Fluorescence emission was measured at 90° to the excitation beam with a long-pass 455 nm filter placed at the entrance slit of the spectrograph. Sample integrity was examined by observing real-time photon counts that, if constant, indicates the absence of sample photodegradation. In order to minimize sample decomposition, TRF studies were performed on the HPLC-eluted sample in the solvent mixture.

### Data processing and global analysis

Prior to analysis, TA datasets were corrected for temporal dispersion using Surface Xplorer 4.0 (UltrafastSystems LLC). The datasets were globally fitted with a kinetic model assuming a sequential population of excited states/species in a cascade of nonreversible, decreasing rates (longer lifetimes). The instrument response function (IRF) was simulated by a Gaussian with a full width at half-maximum (FWHM) of ~200 fs. The fitting procedure used to TA datasets gives EADS – evolution associated difference spectra (44). According to this model, the TA signal at any time delay and wavelength,  $\Delta A(t, \lambda)$ , can be reconstructed from superposition of  $n^{\text{th}}$   $C_i(t)$  and  $\text{EADS}_i(\lambda)$  products

$$\Delta A(t, \lambda) = \sum_{i=1}^n C_i(t) \text{EADS}_i(\lambda) \quad (2)$$

$C_i(t)$ , is time-dependent concentration of  $i^{\text{th}}$  EADS is expressed as

$$\frac{dC_i(t)}{dt} = k_{i-1}C_{i-1}(t) - k_iC_i(t), i \neq 1, k_{i-1} > k_i \quad (3)$$

and  $C_1(t)$ , is populated by the excitation pulse that in spectrometer is represented as instrument response function, IRF:

$$\frac{dC_1(t)}{dt} = \text{IRF}(t) - k_1 C_1(t) \quad (4)$$

Global analysis of TRF data included customized fitting model (target analysis) which assumed more complicated (customized) interactions between compartments. The model used to fit the TRF data is provided as an insert in Figure 2B. Global analysis was performed using CarpetView 1.0 (Light Conversion Ltd.). All plots were created in Origin 2019 (OriginLab Corp.).

### **Modeling of the vibronic progression of fluorescence emission spectrum with Franck-Condon (FC) factors**

Upon assumption that vibronic progression of the fluorescence spectrum is dominated with some average vibronic mode  $\langle \nu \rangle$  with average displacement  $\langle \Delta \rangle$  the F-C equation:

$$FC(\nu) = C\nu \sum_v \prod_i \frac{\Delta_i^{2v}}{2^v v!} \exp\left(-\frac{\Delta_i^2}{2}\right) \frac{1}{2\pi\sigma} \exp\left\{-\frac{[\nu - (\nu_{00} - \sum_i \nu \nu_i)]^2}{2\sigma^2}\right\} \quad (5)$$

simplifies to the following form:

$$FC(\nu) = C\nu \sum_v \frac{\langle \Delta \rangle^{2v}}{2^v v!} \exp\left(-\frac{\langle \Delta \rangle^2}{2}\right) \frac{1}{2\pi\sigma} \exp\left\{-\frac{[\nu - (\nu_{00} - \nu \langle \nu \rangle)]^2}{2\sigma^2}\right\} \quad (6)$$

Where C is the scaling constant,  $\nu$  is the number of vibronic bands included in the progression,  $\sigma$  is the width of the vibronic band (in  $\text{cm}^{-1}$ ) and  $\nu_{00}$  is (in this case) energy of the  $S_1$  state (in  $\text{cm}^{-1}$ ) of  $\zeta$ -carotene.

### **Data Availability**

All data needed to support the conclusions of this manuscript are included in the main text and SI Appendix. *Rhodobacter sphaeroides* strains are available upon request.

### Acknowledgements

Spectroscopic work was performed at the Ultrafast Laser Facility of the Center for Solar Energy and Energy Storage at Washington University in Saint Louis. D.M.N. acknowledges the Center for Solar Energy and Energy Storage at McKelvey School of Engineering at Washington University in Saint Louis for financial support. D.J.K.S., D.P.C., C.N.H. and A.H. were supported by the Biotechnology and Biological Sciences Research Council (BBSRC UK) award number BB/M000265/1. A.H. also acknowledges support from a Royal Society University Research Fellowship (award number URF\R1\191548).

### References

1. R. J. Cogdell, H. A. Frank, How carotenoids function in photosynthetic bacteria. *Biochim. Biophys. Acta* **895**, 63-79 (1987).
2. H. A. Frank, T. Polívka, "Energy transfer from carotenoids to bacteriochlorophylls" in *The Purple Phototrophic Bacteria*, C. N. Hunter, F. Daldal, M. Thurnauer, J. T. Beatty, Eds. (Springer Netherlands, 2009), vol. 28, chap. 12, pp. 213-230.
3. B. E. Kohler, "Electronic structure of carotenoids" in *Carotenoids*, G. Britton, S. Liaaen-Jensen, H. Pfander, Eds. (Birkhäuser-Verlag Basel, 1995), vol. 1B Spectroscopy, pp. 3–12.
4. H. Hashimoto, C. Uragami, N. Yukihiro, A. T. Gardiner, R. J. Cogdell, Understanding/unravelling carotenoid excited singlet states. *J. R. Soc. Interface* **15** (2018).
5. R. J. Cogdell et al., How carotenoids protect bacterial photosynthesis. *Philos. Trans. R. Soc. B* **355**, 1345–1349 (2000).
6. T. Polívka, H. A. Frank, Molecular factors controlling photosynthetic light harvesting by carotenoids. *Acc. Chem. Res.* **43**, 1125–1134 (2010).
7. Y. Kakitani et al., Conjugation-length dependence of the  $T_1$  lifetimes of carotenoids free in solution and incorporated into the LH2, LH1, RC, and RC-LH1 complexes: Possible mechanisms of triplet-energy dissipation. *Biochemistry* **46**, 2181–2197 (2007).
8. H. H. Billsten et al., Dynamics of energy transfer from lycopene to bacteriochlorophyll in genetically-modified LH2 complexes of *Rhodobacter sphaeroides*. *Biochemistry* **41**, 4127–4136 (2002).

9. J. P. Zhang et al., Mechanism of the carotenoid-to-bacteriochlorophyll energy transfer via the  $S_1$  state in the LH2 complexes from purple bacteria. *J. Phys. Chem. B* **104**, 3683–3691 (2000).
10. A. N. Macpherson, J. B. Arellano, N. J. Fraser, R. J. Cogdell, T. Gillbro, Efficient energy transfer from the carotenoid  $S_2$  state in a photosynthetic light-harvesting complex. *Biophys. J.* **80**, 923–930 (2001).
11. H. Cong et al., Ultrafast time-resolved carotenoid to-bacteriochlorophyll energy transfer in LH2 complexes from photosynthetic bacteria. *J. Phys. Chem. B* **112**, 10689–10703 (2008).
12. F. S. Rondonuwu et al., The role of the  $1^1B_u^-$  state in carotenoid-to-bacteriochlorophyll singlet-energy transfer in the LH2 antenna complexes from *Rhodobacter sphaeroides* G1C, *Rhodobacter sphaeroides* 2.4.1, *Rhodospirillum molischianum* and *Rhodopseudomonas acidophila*. *Chem. Phys. Lett.* **390**, 314–322 (2004).
13. D. M. Niedzwiedzki et al., Spectroscopic studies of two spectral variants of light-harvesting complex 2 (LH2) from the photosynthetic purple sulfur bacterium *Allochromatium vinosum*. *BBA-Bioenergetics* **1817**, 1576–1587 (2012).
14. D. M. Niedzwiedzki et al., Functional characteristics of spirilloxanthin and keto-bearing Analogues in light-harvesting LH2 complexes from *Rhodobacter sphaeroides* with a genetically modified carotenoid synthesis pathway. *BBA-Bioenergetics* **1847**, 640–655 (2015).
15. D. M. Niedzwiedzki, M. Fuciman, M. Kobayashi, H. A. Frank, R. E. Blankenship, Ultrafast time-resolved spectroscopy of the light-harvesting complex 2 (LH2) from the photosynthetic bacterium *Thermochromatium tepidum*. *Photosynth. Res.* **110**, 49–60 (2011).
16. F. Yang et al., Excitation dynamics of the light-harvesting complex 2 from *Thermochromatium tepidum*. *Acta Phys.-Chim. Sin.* **26**, 2021–2030 (2010).
17. J. Koepke, X. C. Hu, C. Muenke, K. Schulten, H. Michel, The crystal structure of the light-harvesting complex II (B800-850) from *Rhodospirillum molischianum*. *Structure* **4**, 581–597 (1996).
18. S. M. Prince et al., Apoprotein structure in the LH2 complex from *Rhodopseudomonas acidophila* strain 10050: modular assembly and protein pigment interactions. *J. Mol. Biol.* **268**, 412–423 (1997).
19. S. C. Chi et al., Assembly of functional photosystem complexes in *Rhodobacter sphaeroides* incorporating carotenoids from the spirilloxanthin pathway. *BBA-Bioenergetics* **1847**, 189–201 (2014).
20. D. M. Niedzwiedzki et al., New insights into the photochemistry of carotenoid spheroidenone in light-harvesting complex 2 from the purple bacterium *Rhodobacter sphaeroides*. *Photosynth. Res.* **131**, 291–304 (2017).
21. D. M. Niedzwiedzki, C. N. Hunter, R. E. Blankenship, Evaluating the nature of so-called  $S^*$ -state feature in transient absorption of carotenoids in light-harvesting complex 2 (LH2) from purple photosynthetic bacteria. *J. Phys. Chem. B* **120**, 11123–11131 (2016).
22. P. L. Dilbeck et al., Quenching capabilities of long-chain carotenoids in light harvesting-2 complexes from *Rhodobacter sphaeroides* with an engineered carotenoid synthesis pathway. *J. Phys. Chem. B* **120**, 5429–5443 (2016).

23. R. J. Cogdell, M. F. Hipkins, W. Macdonald, T. G. Truscott, Energy-transfer between the carotenoid and the bacteriochlorophyll within the B800-850 light-harvesting pigment-protein complex of *Rhodospseudomonas sphaeroides*. *Biochim. Biophys. Acta* **634**, 191–202 (1981).
24. A. Angerhofer, F. Bornhauser, A. Gall, R. J. Cogdell, Optical and optically detected magnetic-resonance investigation on purple photosynthetic bacterial antenna complexes. *Chem. Phys.* **194**, 259–274 (1995).
25. H. A. Frank, R. J. Cogdell, Carotenoids in photosynthesis. *Photochem. Photobiol.* **63**, 257–264 (1996).
26. A. Angerhofer, R. J. Cogdell, M. F. Hipkins, A spectral characterization of the light-harvesting pigment-protein complexes from *Rhodospseudomonas acidophila*. *Biochim. Biophys. Acta* **848**, 333–341 (1986).
27. D. Polli et al., Carotenoid-bacteriochlorophyll energy transfer in LH2 complexes studied with 10-fs time resolution. *Biophys. J.* **90**, 2486–2497 (2006).
28. M. M. Mendes-Pinto et al., Electronic absorption and ground state structure of carotenoid molecules. *J. Phys. Chem. B* **117**, 11015–11021 (2013).
29. M. Fuciman et al., Excited state properties of aryl carotenoids. *Phys. Chem. Chem. Phys.* **12**, 3112–3120 (2010).
30. D. M. Niedzwiedzki, L. Cranston, Excited state lifetimes and energies of okenone and chlorobactene, exemplary keto and non-keto aryl carotenoids. *Phys. Chem. Chem. Phys.* **17**, 13245–13256 (2015).
31. R. Bittl, E. Schlodder, I. Geisenheimer, W. Lubitz, R. J. Cogdell, Transient EPR and absorption studies of carotenoid triplet formation in purple bacterial antenna complexes. *J. Phys. Chem. B* **105**, 5525–5535 (2001).
32. D. Kosumi, T. Horibe, M. Sugisaki, R. J. Cogdell, H. Hashimoto, Photoprotection mechanism of light-harvesting antenna complex from purple bacteria. *J. Phys. Chem. B* **120**, 951–956 (2016).
33. D. A. Hartzler et al., Triplet excited state energies and phosphorescence spectra of (Bacterio)chlorophylls. *J. Phys. Chem. B* **118**, 7221–7232 (2014).
34. C. S. Foote, Y. C. Chang, R. W. Denny, Chemistry of singlet oxygen. X. Carotenoid quenching parallels biological protection. *J. Am. Chem. Soc.* **92**, 5216–5218 (1970).
35. H. Claes, Interaction between chlorophyll and carotenes with different chromophoric groups. *Biochem. Biophys. Res. Commun.* **3**, 585–590 (1960).
36. R. Bensasson, E. J. Land, B. Maudinas, Triplet states of carotenoids from photosynthetic bacteria studied by nanosecond ultraviolet and electron pulse irradiation. *Photochem. Photobiol.* **23**, 189–193 (1976).
37. E. Papagiannakis et al., Excited-state dynamics of carotenoids in light-harvesting complexes. 1. Exploring the relationship between the  $S_1$  and  $S^*$  states. *J. Phys. Chem. B* **110**, 5727–5736 (2006).
38. R. Fujii, K. Onaka, M. Kuki, Y. Koyama, Y. Watanabe, The  $2A_g^-$  energies of all-trans-neurosporene and spheroidene as determined by fluorescence spectroscopy. *Chem. Phys. Lett.* **288**, 847–853 (1998).
39. C. N. Hunter, G. Turner, Transfer of genes-coding for apoproteins of reaction center and light-harvesting LH1 complexes to *Rhodobacter sphaeroides*. *J. Gen. Microbiol.* **134**, 1471–1480 (1988).

40. I. B. Tikh, M. Held, C. Schmidt-Dannert, BioBrick(TM) compatible vector system for protein expression in *Rhodobacter sphaeroides*. *Appl. Microbiol. Biot.* **98**, 3111-3119 (2014).
41. D. J. K. Swainsbury et al., Engineering of B800 bacteriochlorophyll binding site specificity in the *Rhodobacter sphaeroides* LH2 antenna. *BBA-Bioenergetics* **1860**, 209-223 (2019).
42. D. M. Niedzwiedzki et al., Carotenoid-induced non-photochemical quenching in the cyanobacterial chlorophyll synthase-HliC/D complex. *BBA-Bioenergetics* **1857**, 1430-1439 (2016).
43. D. M. Niedzwiedzki, J. Jiang, C. S. Lo, R. E. Blankenship, Low-temperature spectroscopic properties of the peridinin-chlorophyll a-protein (PCP) complex from the coral symbiotic dinoflagellate *Symbiodinium*. *J. Phys. Chem. B* **117**, 11091-11099 (2013).
44. I. H. M. van Stokkum, D. S. Larsen, R. van Grondelle, Global and target analysis of time-resolved spectra. *BBA-Bioenergetics* **1657**, 82-104 (2004).

## Figure Legends

**Figure 1.** Spectroscopic comparison of the  $\zeta$ -carotene-containing LH2 antenna complex from *Rba. sphaeroides* and all-trans- $\zeta$ -carotene in solvent at room temperature. The chemical structure of the Car is shown above the panels. The C=C bonds highlighted in red indicate the conjugation length ( $N = 7$ ) of the Car. (A) Comparison between absorbance (black) and fluorescence excitation (red) spectra shows that in LH2  $\zeta$ -carotene transfers excitation energy to BChl a essentially without any energetic loss. (B) All-trans- $\zeta$ -carotene dissolved in solvent shows pronounced fluorescence emission from the  $S_1$  state and a much weaker emission band from the  $S_2$  state.

**Figure 2.** Time-resolved fluorescence (TRF) of all-trans- $\zeta$ -carotene in solvent upon excitation at 410 nm at room temperature. (A) Pseudo-color contour of TRF with the  $S_2 \rightarrow S_0$  and  $S_1 \rightarrow S_0$

transitions indicated. (B) Global analysis results (SAS – species associated spectra) from application of fitting model depicted in the panel. The SAS are normalized to their maximal time-dependent concentrations. A small contribution of the long-lived (1.6 ns) component was also necessary to properly fit the TRF data, which most likely originates from a decomposition product that slowly accumulates during measurements. (C) Fluorescence dynamics for two exemplary wavelengths accompanied with fits. (D) Simulation of the  $S_1 \rightarrow S_0$  fluorescence spectrum, approximated by the 340 ps SAS from panel B, with F-C progression. For more details please refer to the text. Simulation places the  $S_1$  state energy at  $\sim 18,000 \text{ cm}^{-1}$  (555 nm).

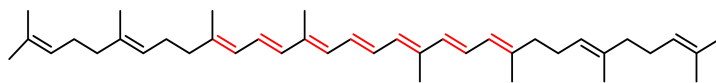
**Figure 3.** Room temperature transient absorption of  $\zeta$ -carotene-containing LH2 from Rba. sphaeroides upon excitation of the Car absorption band. (A) 2D pseudo-color contour of TA with spectral features marked. (B) Representative TA spectra taken at various delay times after excitation at the (0-0) vibronic band of the  $S_0 \rightarrow S_2$  absorption of  $\zeta$ -carotene. (C) Example TA time courses recorded at selected wavelengths. (D) Evolution associated decay spectra (EADS) with application of a sequential decay model. The insert in panel D represents a zoomed-in view of the  $Q_x$  band. GSB - ground state bleaching; ESA – excited state absorption.

**Figure 4.** Transient absorption of the  $\zeta$ -carotene-containing LH2 complex over a  $\mu\text{s}$  time range and comparison with neurosporene-containing LH2. (A, B) Pseudo-color contours of the TA for both LH2 complexes obtained after excitation of the Car band. Noticeable transient bands are marked. (C, D) Individual TA spectra recorded at various delay times after the excitation. The

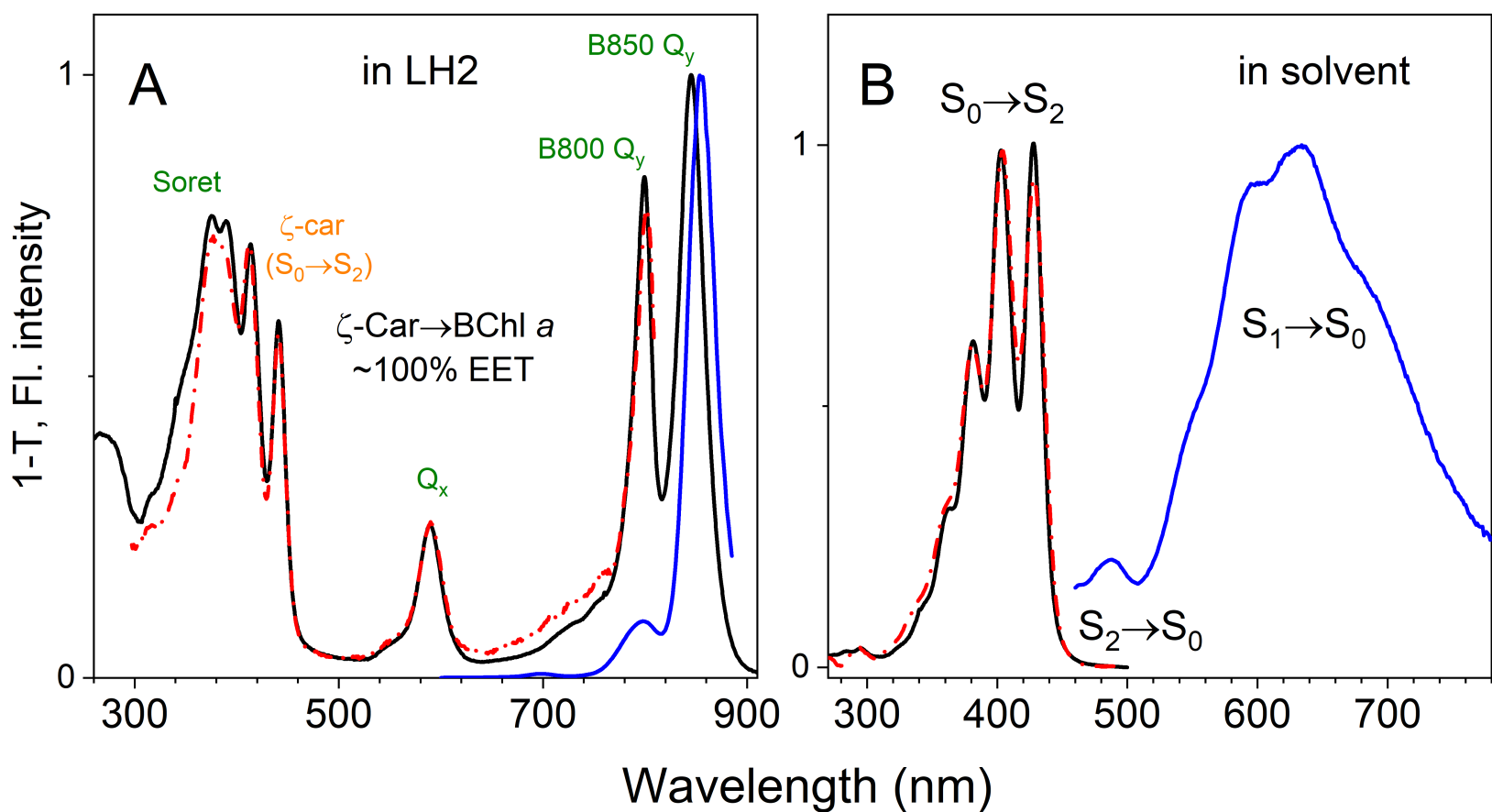


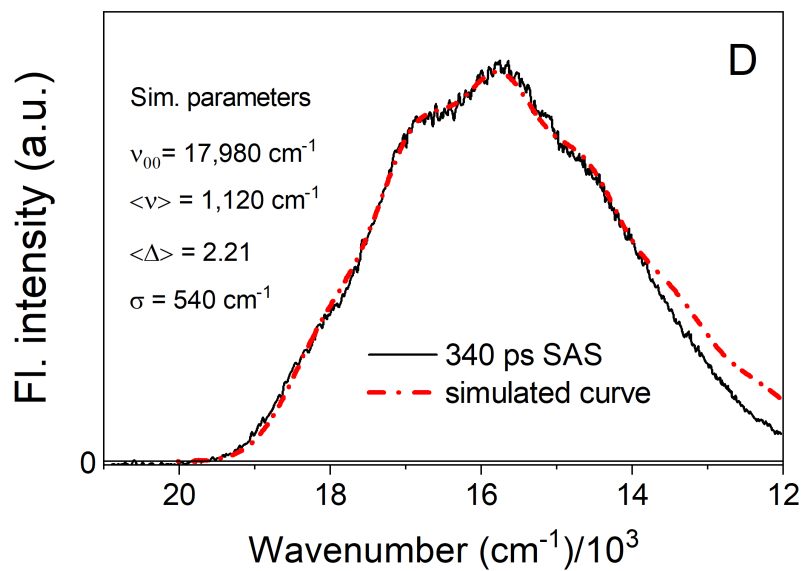
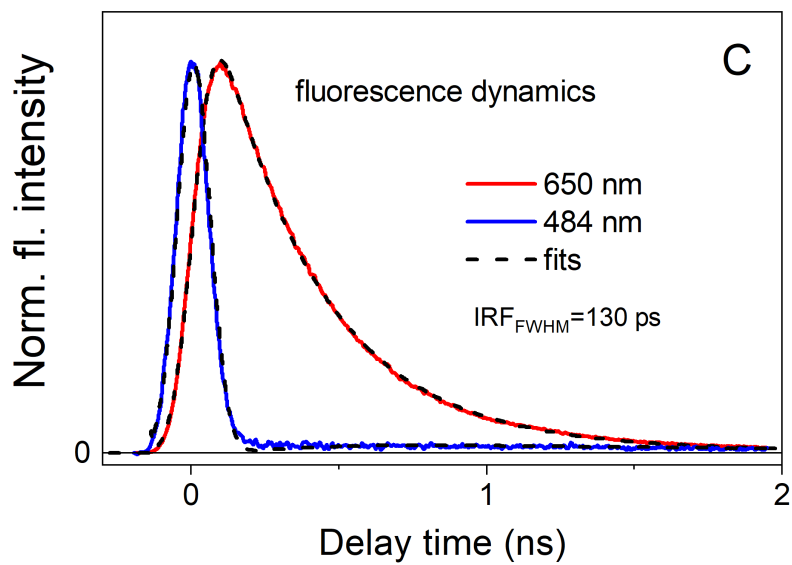
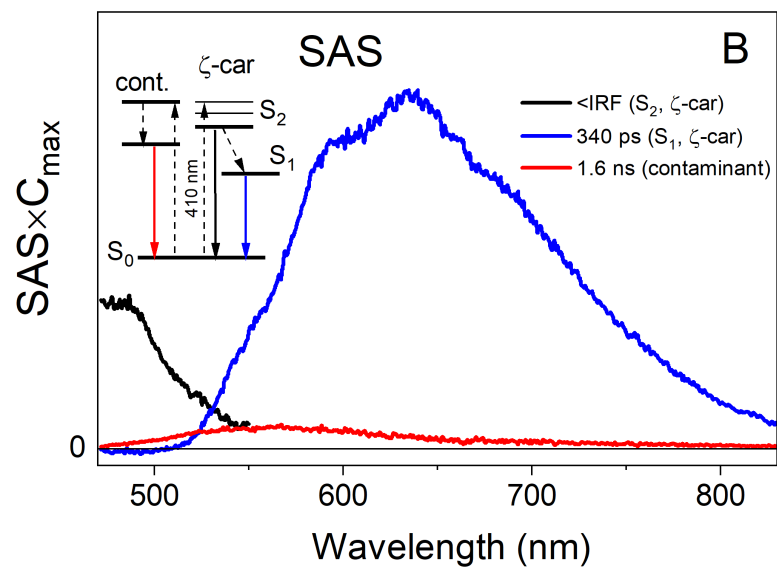
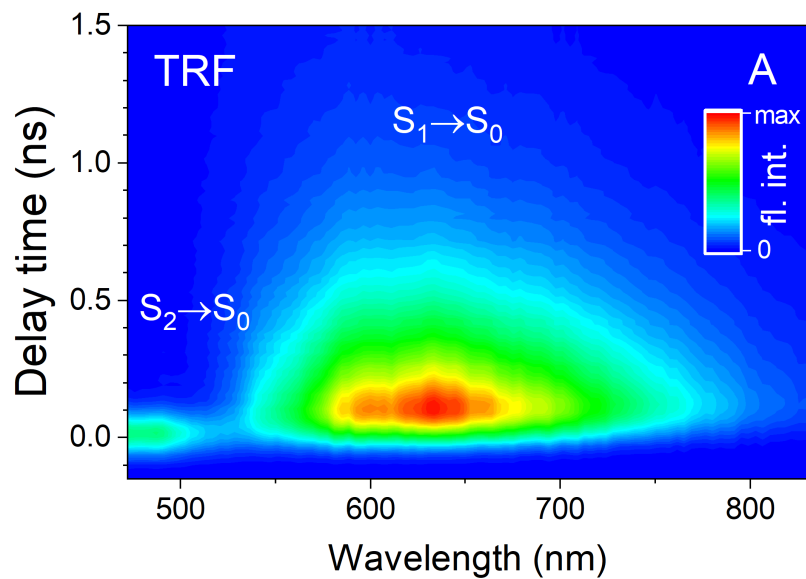
inserts show TA in the spectral range in which triplet-minus-singlet (T-S) spectra of the carotenoid appear. (E, F) Representative TA kinetic traces recorded at the bleaching of B850  $Q_y$  band (852 and 868 nm) and at the maximum of the Car  $T_1 \rightarrow T_n$  ESA band (507 nm, neurosporene-LH2 only). For clarity, time delays are plotted on a log scale and are slightly offset from  $t_0=0$ .

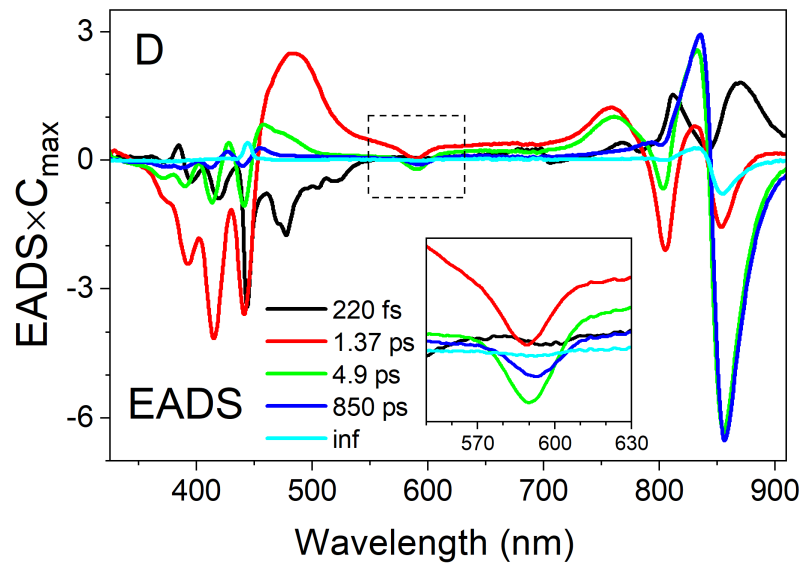
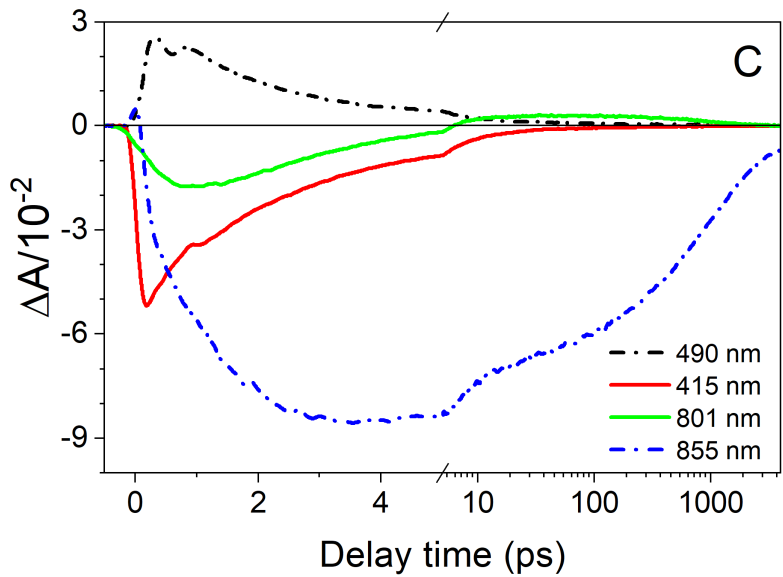
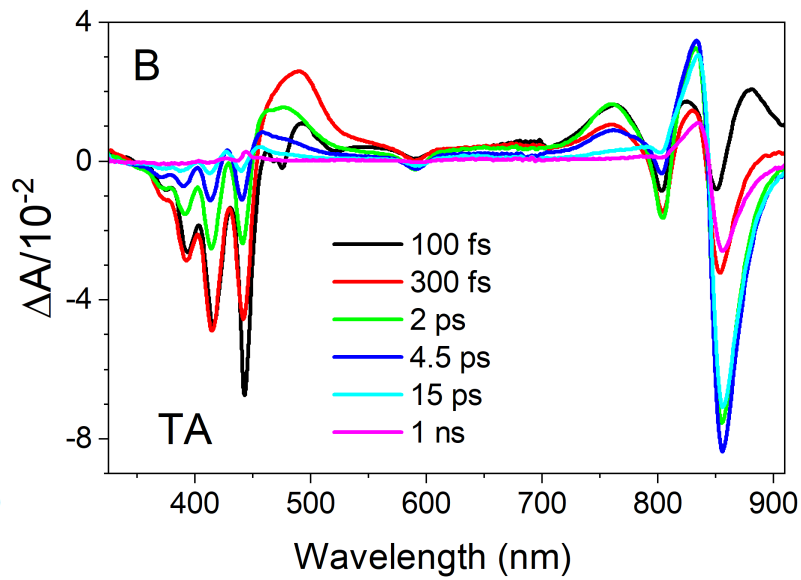
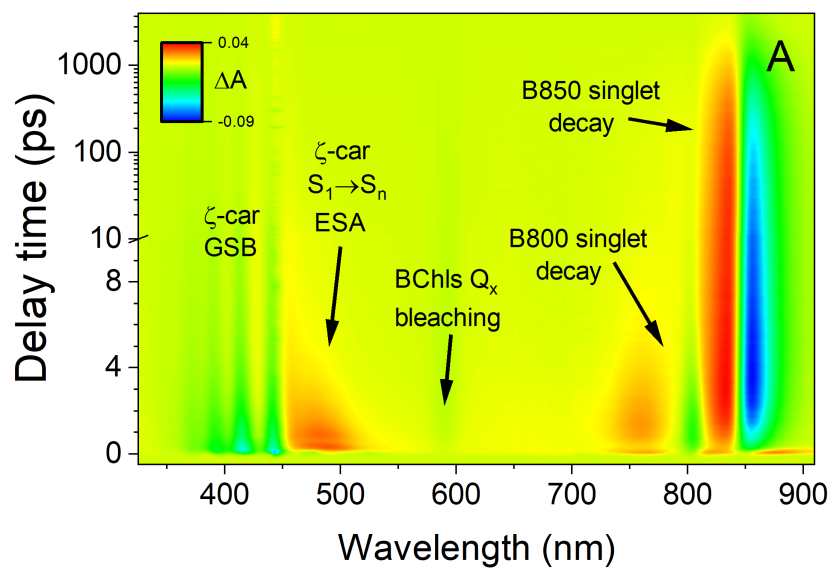
all-trans  
 $\zeta$ -carotene ( $N = 7$ )

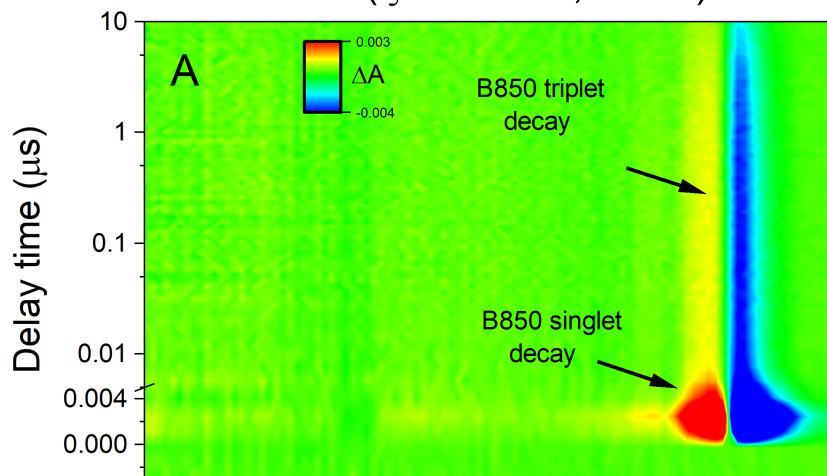
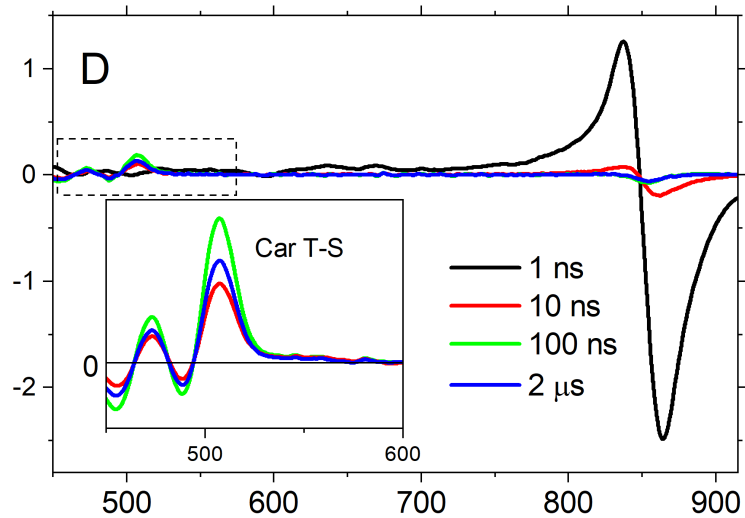
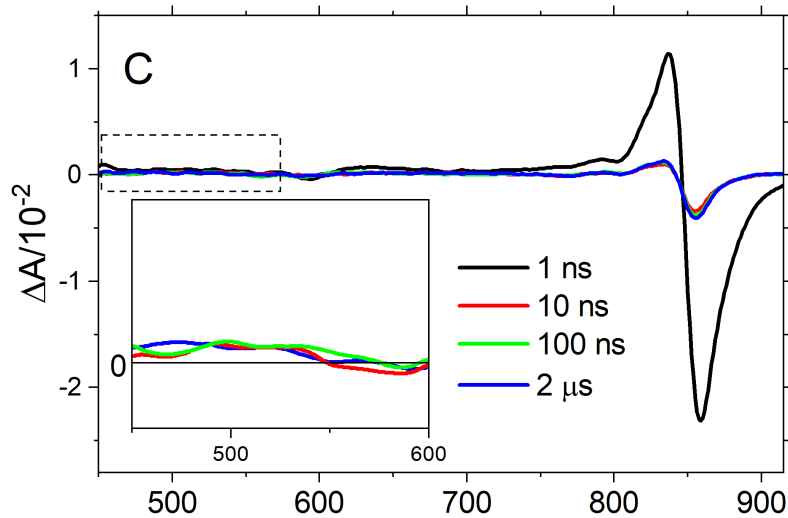
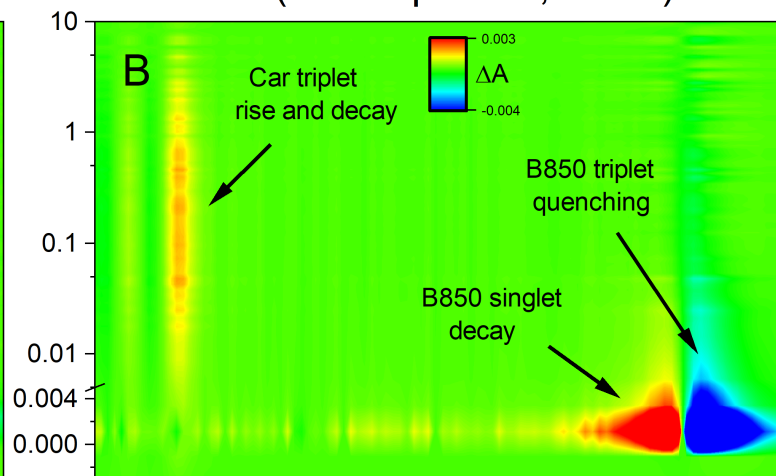


— Absorbance (1-T)  
- · - Fluo. excitation  
— Fluo. emission

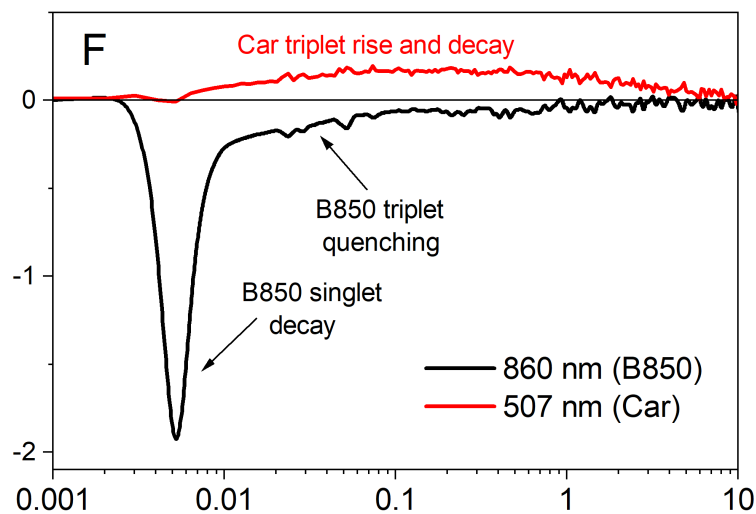
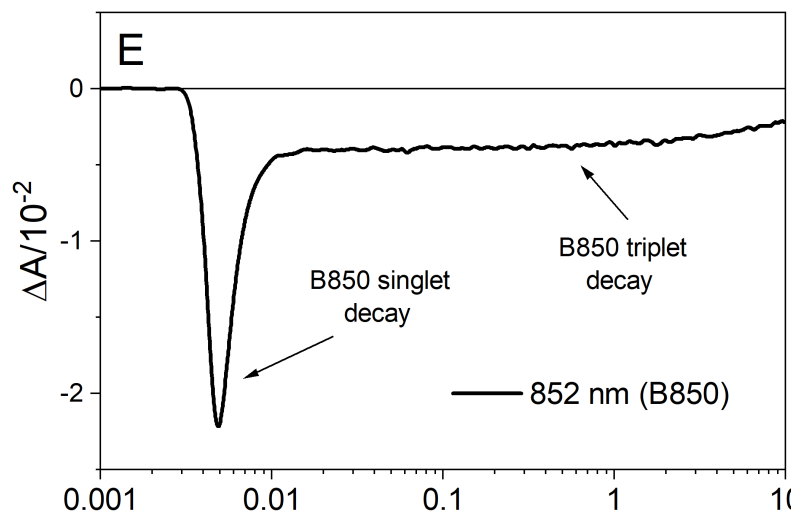






LH2 ( $\zeta$ -carotene,  $N = 7$ )LH2 (neurosporene,  $N = 9$ )

Wavelength (nm)

Time delay ( $\mu\text{s}$ )